UNIABUJA Journal of Engineering and Technology
https://ujet.uniabuja.edu.ng/
ISSN: 2714-3236 (Online); 2714-3228 (Print)
Volume 3, Issue 2, 2026; 365-374

An Explainable AI-Based Computer Vision Framework for Printed Circuit Board Defect Detection Using YOLOv4

Hamed B. FOLORUNSHO[1*], Ukoh J. SAMUEL[1], Abayomi I.O. YUSSUFF[1], Olatunde A. OGUNDEJI[2], Ayangbenjo H. ADEYEYE[2]

[1] Department of Electronics and Computer Engineering, Lagos State University, Epe Campus
[2] Department of Electrical and Electronics Engineering, Adeseun Ogundoyin Polytechnic, Eruwa, Oyo State

[1*]hamed.folorunsho@lasu.edu.ng, [2]olatunde.ogundeji@aope.edu.ng

Abstract
Printed Circuit Boards (PCBs) are critical components in modern electronic systems, where manufacturing defects can significantly compromise device reliability, safety, and operational performance. Conventional inspection techniques, including manual inspection and traditional Automated Optical Inspection (AOI), are often limited by subjectivity, high operational cost, and reduced scalability. This study proposes a lightweight and explainable Artificial Intelligence (AI)-based computer vision framework for automated PCB defect detection using a YOLOv4 object detection model integrated with multimodal explainable Artificial Intelligence (AI). A publicly available annotated PCB dataset sourced from Roboflow Universe was utilized for model training and evaluation, with data augmentation techniques including rotation, brightness adjustment, cropping, flipping, and noise injection applied to improve model robustness. The trained YOLOv4 model achieved a precision of 91.4%, recall of 87.8%, and mAP@0.5 of 89.2% with an average inference time of approximately 80 ms per image. To improve interpretability and usability, Gemini AI was integrated to generate natural-language explanations, defect summaries, and repair-oriented guidance based on detected anomalies. The complete framework was deployed as a responsive web-based application using Next.js, TailwindCSS, Prisma ORM, and PostgreSQL, supporting both single-image and batch-image inspection workflows. Experimental results demonstrate that the proposed system provides accurate, fast, and interpretable PCB defect inspection while maintaining accessibility for small-scale manufacturing, educational, and research environments. The study highlights the potential of integrating deep learning and explainable AI for scalable and cost-effective intelligent inspection systems in modern electronics manufacturing.

Keywords: *Printed Circuit Boards, PCB defect detection, YOLOv4, computer vision, explainable artificial intelligence, automated optical inspection, deep learning.*

1.0 Introduction

Printed Circuit Boards (PCBs) serve as the mechanical and electrical backbone of modern electronic systems by interconnecting active and passive components through conductive copper traces embedded within insulating substrates (Ike-Eze et al., 2023: Kowalke et al., 2024). Their applications span consumer electronics, aerospace, healthcare, industrial automation, and telecommunications, making PCB reliability critical to the safety and performance of contemporary devices (Silvestre et al., 2019, Shamkhalichenar et al., 2020). However, manufacturing defects such as solder bridges, broken traces, spurious copper, and open circuits can significantly degrade system functionality, reduce product lifespan, and trigger costly recalls if not detected during production (Sankar et al., 2022; Nayak et al., 2017). Consequently, accurate and early-stage defect inspection has become an essential aspect of modern electronics manufacturing.

Conventional PCB inspection techniques include manual visual inspection, electrical testing, Automated Optical Inspection (AOI), and Automated X-ray Inspection (AXI). Manual inspection is slow, subjective, and highly dependent on technician expertise, while electrical testing requires customized circuits that increase cost and complexity. AOI systems improved inspection through non-contact optical imaging and automated defect analysis by Qiu et al. (2024) and Liao et al. (2018), but they remain expensive and are primarily limited to surface-level inspection (Zakaria et al., 2020). Similarly, AXI systems enable the detection of hidden solder joint and multilayer defects in complex packages such as BGAs and QFNs, although their high operational cost restricts widespread adoption (Qiu et al., 2024). These limitations have created a growing demand for intelligent, scalable, and cost-effective PCB inspection solutions suitable for both industrial and academic environments.

Recent advances in computer vision and deep learning have significantly improved PCB defect detection performance. Convolutional Neural Networks (CNNs) and deep learning-based object detection methods have demonstrated strong capabilities in identifying subtle PCB anomalies with high accuracy (Park et al., 2023; Pham et al., 2023; Kim et al., 2021; Cheng et al., 2022; Hao et al., 2023). Among these approaches, YOLO-based architectures have gained prominence because of their ability to achieve real-time detection with high

Received: 12-07-2026 / Accepted: 23-07-2026 / Published: 07-09-2026

https://doi.org/10.70118/ujet.2026.0302.31

precision (Redmon et al., 2016). Variants such as YOLOv5, YOLOv7, and YOLOv8 have shown excellent performance on PCB benchmark datasets, while lightweight and ensemble-based adaptations further improve efficiency and deployment on resource-constrained devices (Law et al., 2024; Wang et al., 2025). Despite these deep learning advances, many existing inspection architectures still require expensive proprietary hardware or advanced technical expertise, limiting their practical adoption in small-scale manufacturing and academic environments (Law et al., 2024; Arrieta et al., 2020). Furthermore, standard object detection models operate as black boxes outputting bounding boxes without explaining the operational severity of defects or how to fix them (Arrieta et al., 2020).

To address these limitations, this study proposes a lightweight and explainable AI-driven PCB defect detection framework that integrates a YOLO-based object detection model with a dedicated Explainable AI (XAI) and Natural Language Processing (NLP) layer (Roboflow, 2025; Google DeepMind, 2025). The system utilizes accessible cloud-based training infrastructure through Roboflow (Roboflow, 2025) and incorporates the Gemini multimodal language model (Google DeepMind, 2025) as an XAI pipeline. This pipeline translates spatial bounding box coordinates and classification metadata into natural-language defect explanations, operational severity assessments, and step-by-step repair guidance (Google DeepMind, 2025). By combining accurate defect localization with interpretable, actionable diagnostics, the proposed framework provides an accessible and cost-effective alternative for small-scale electronics manufacturers, repair technicians, and educational institutions (Ike-Eze et al., 2023; Google DeepMind, 2025).

2.0 Materials and Methods

2.1 System Architecture

The proposed PCB defect detection framework was designed as a modular artificial intelligence pipeline integrating object detection, visualization, explainable AI, and web-based interaction. The system architecture comprises five major components: a Next.js frontend interface, a backend API layer integrated with Prisma ORM, a YOLOv4-based defect detection model hosted on Roboflow, the Gemini multimodal language model for interpretability, and a PostgreSQL database for persistent data storage. Figure 1 presents the workflow of the system architecture, the process begins with user-uploaded PCB images, which are transmitted through secure API routes to the Roboflow inference engine for defect localization and classification. The returned predictions, including bounding boxes, class labels, and confidence scores, are further processed for visualization and natural-language interpretation before being rendered to the user interface.

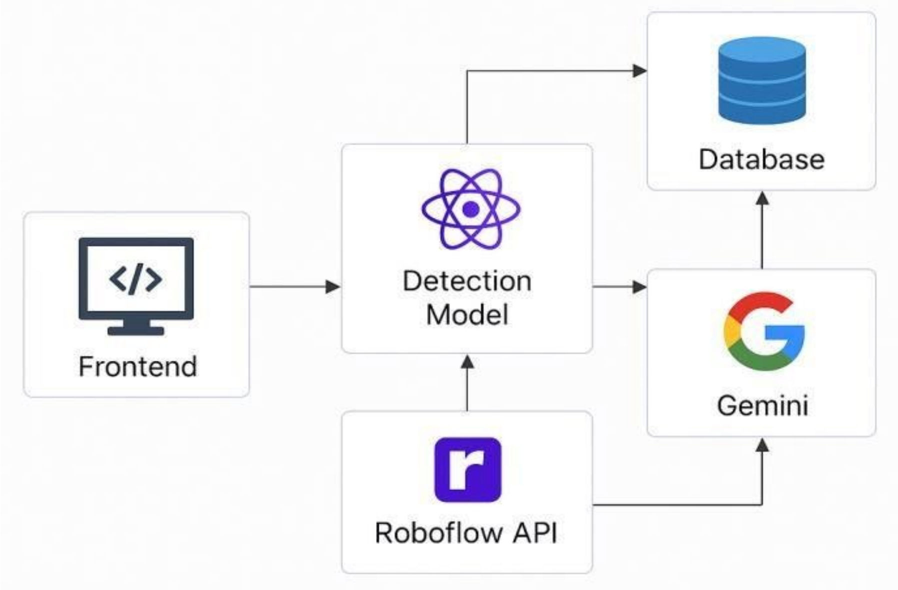

Figure 1: System architecture of the proposed PCB defect detection framework.

2.2 Dataset Collection and Pre-processing

The dataset used in this study was acquired from the Roboflow Universe repository (Roboflow, 2025). It comprises 1,320 high-resolution PCB images containing 2,868 annotated defect instances across five common manufacturing classes: Open Circuit, Short Circuit, Missing Hole, Mouse Bite, and Spurious Copper. The dataset was split using a standard 70:20:10 ratio, resulting in 924 images for training, 264 images for validation, and 132 images for testing. All defect bounding boxes were formatted and stored using the standard YOLO Darknet annotation format (normalized center coordinates x, y along with width (w) and height (h) relative to image dimensions) (Bochkovskiy et al., 2020). Image dimensions were resized and standardized to 416×416 pixels during preprocessing to match the input layer requirements of the YOLOv4 architecture

Received: 12-07-2026 / Accepted: 23-07-2026 / Published: 07-09-2026
https://doi.org/10.70118/ujet.2026.0302.31

(Bochkovskiy et al., 2020). Table 1 summarizes representative PCB defects, their descriptions, and visual characteristics (Sankar et al., 2022; Nayak et al., 2017).

2.3 Model Training and Deployment

The YOLOv4 architecture was selected for this framework due to its optimal balance between detection precision and real-time inference speed on resource-constrained web interfaces (Bochkovskiy et al., 2020). While newer architectures exist (e.g., YOLOv7 or YOLOv8), YOLOv4 provides superior model stability, a lightweight memory footprint suitable for cloud API microservices, and high capability in detecting small spatial features typical of PCB defects through its CSPDarknet53 backbone and PANet path-aggregation neck (Wang et al., 2022; Wang et al., 2025, (Bochkovskiy et al., 2020). Training was performed using the Roboflow GPU-accelerated cloud training engine with the model variant pcb-defect-detection-fyopy/4. The model was trained for a maximum of 100 epochs. During training, early stopping was employed to prevent overfitting.

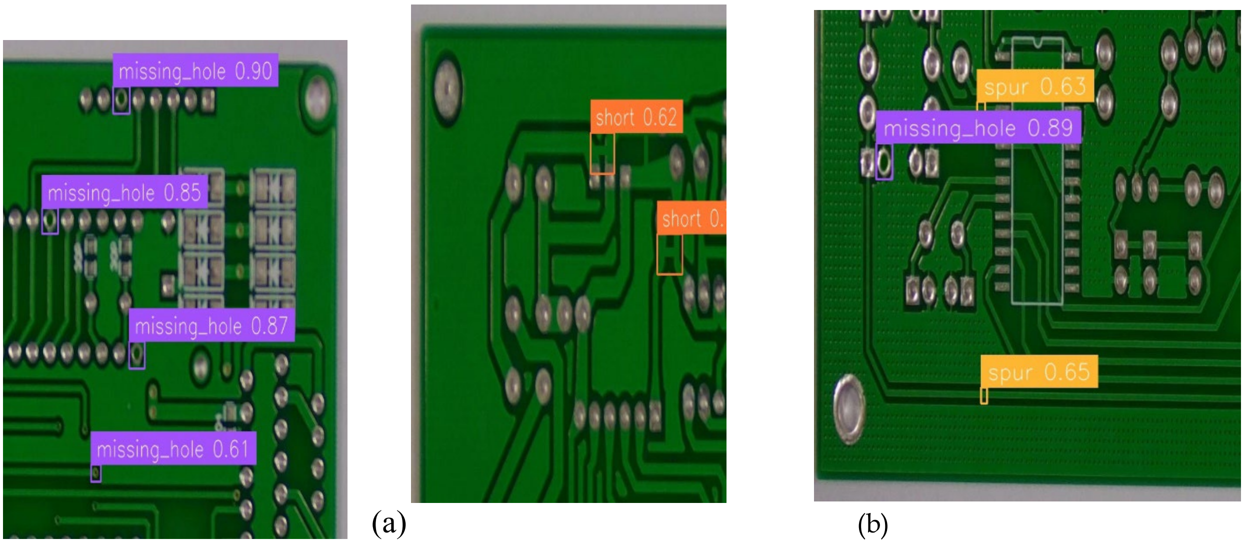

(a) (b) (c)

Figure 2: PCB defect images: (a) Missing Hole (b) Short Circuit (c) Spurious Copper

Table 1: Representative PCB defects and visual characteristics.

Defect Type	Description	Visual Cue
Open Circuit	Break in the trace	Thin gap between copper lines
Spurious Copper	Unwanted copper paths	Random thin copper lines
Mouse Bite	Jagged or irregular drill holes	Rough circular voids
Missing Hole	Missing or incomplete drilled hole	Absence of drill location

The training process terminated automatically after 62 epochs when no significant improvement in validation performance was observed. Performance evaluation was conducted using precision, recall, mean Average Precision (mAP@0.5), and inference time. The final trained model achieved approximately 89.2% mAP@0.5 on the test set. After training, the model was deployed through the Roboflow Inference API and integrated into the application back-end using secure API authentication. Table 2 include YOLOv4 Training Configuration.

Table 2: YOLOv4 Training Configuration.

Parameter	Value
Model	YOLOv4
Training Platform	Roboflow
Epochs	100
Early Stopping Epoch	62

Received: 12-07-2026 / Accepted: 23-07-2026 / Published: 07-09-2026

https://doi.org/10.70118/ujet.2026.0302.31

Input Image Size	416×416
Confidence Threshold	0.5
IoU Threshold	0.5
Evaluation Metric	mAP@0.5
Detection Classes	5

2.4 Visualization and Explainability Pipeline

The inference output from YOLOv4 was processed through a visualization layer to improve interpretability. Figure 3 presents the complete detection and explainability workflow, illustrating the transition from image upload and YOLO-based detection to Gemini-assisted interpretation and frontend visualization. The predicted defects were highlighted using bounding-box overlays, label annotations, and confidence indicators. Detection metadata was subsequently passed to Gemini-powered explainability pipelines that generated defect descriptions, probable impact assessments, and summarized inspection reports.

Two major interpretation modules were implemented:

i. Defects details: generates defect-specific explanations and potential operational implications.
ii. Detection overview: summarizes the overall PCB inspection outcome in natural language.

The Gemini responses were parsed into structured JSON format for frontend rendering and optional export.

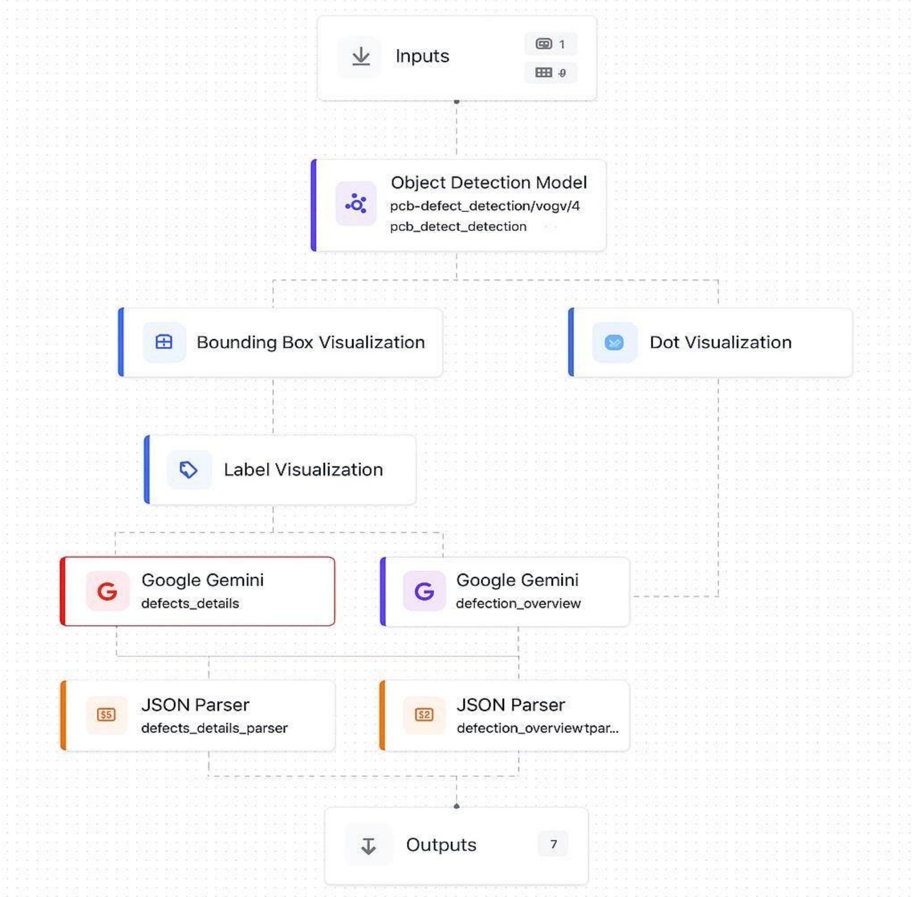

Figure 3: Detection and explainability workflow of the proposed system.

2.5 Application Development

The full-stack application was implemented using Next.js with TailwindCSS for responsive frontend rendering. Backend services were managed through API routes integrated with Prisma ORM and PostgreSQL for storage of scan histories, metadata, and summarized reports. The application supports both single-image and batch-image inspection workflows in Figure 4. Upon image upload, the frontend transmits requests to the back-end inference pipeline, which processes the image, retrieves defect predictions, generates explainable summaries, and returns annotated outputs to the user. Additional functionalities include result visualization, historical scan tracking, export support, and mobile-responsive interaction.

Received: 12-07-2026 / Accepted: 23-07-2026 / Published: 07-09-2026
https://doi.org/10.70118/ujet.2026.0302.31

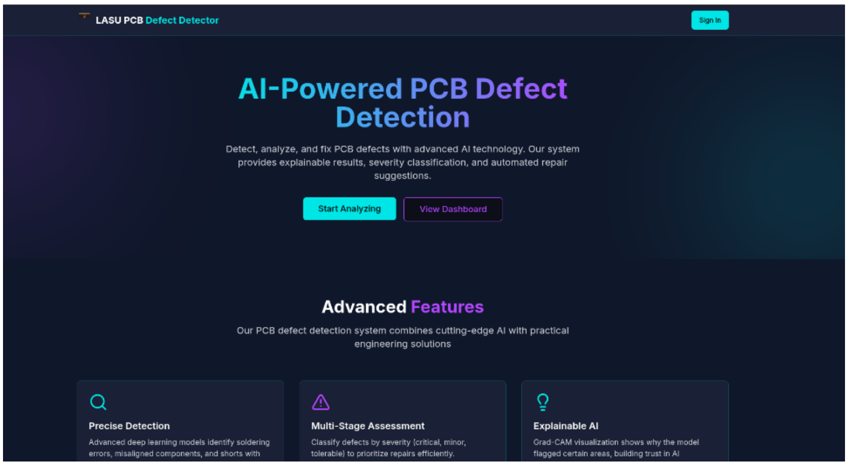

Figure 4: Overview of the application's Front-End interface before user authentication.

3.0 Results and Discussion

3.1 Training Performance

The trained YOLOv4 model achieved a precision of 91.4%, recall of 87.8%, and mAP@0.5 of 89.2%, indicating strong defect localization and classification capability. The high precision value suggests that most detected defects correspond to actual defects, thereby minimizing false alarms during PCB inspection. This characteristic is particularly important in manufacturing environments where excessive false positives can lead to unnecessary product rejection and increased operational costs. The recall value of 87.8% indicates that the majority of defects present in the test dataset were successfully identified. The difference between precision and recall suggests that while the model is highly selective in its predictions, a small number of defects remain undetected under certain imaging conditions. The mAP@0.5 value of 89.2% demonstrates that the detector maintains a high level of localization accuracy across multiple defect classes. This confirms the suitability of YOLOv4 for real-time PCB inspection tasks.

3.2 Detection and Inference Evaluation

The system was evaluated using both previously seen and unseen PCB samples to assess generalization capability under practical operating conditions. The model successfully detected common PCB defects such as missing holes, spurious copper, open circuits, and short circuits with relatively low inference latency. Performance evaluation employed precision, recall, mean Average Precision (mAP@0.5), and inference time. Table 3 presents representative detection results obtained from unseen PCB samples. The results indicate that the proposed framework maintains reliable detection accuracy while preserving near real-time inference performance suitable for practical inspection scenarios.

Table 3: Detection results and inference time for representative PCB test samples.

Metric	Value
Precision	91.4%
Recall	87.8%
mAP@0.5	89.2%
Average Inference Time	~80 ms
FPS	12.5
Detection Accuracy	89.6%
False Positive Rate	8.6%
False Negative Rate	12.2%

To evaluate performance comprehensively, standard object detection metrics (Precision, Recall, mAP@0.5) were complemented by instance-level metric evaluations (Park et al., 2023). Detection Accuracy (89.6%) represents the ratio of correctly localized and classified defect instances relative to total ground-truth defect instances across the unseen test batch. False Positive Rate (FPR = 8.6%) measures the proportion of non-defect regions or background noise incorrectly flagged as defects, directly reflecting model selectivity (Precision = 94.4%). Conversely, False Negative Rate (FNR = 12.2%) indicates undetected real defects (FNR = 1- Recall, where Recall = 87.8%) (Park et al., 2023). These instance-based metrics confirm that the detector maintains high specificity, which is vital in manufacturing settings to prevent over-rejection of acceptable PCBs.

Table 4: Performance evaluation metrics of the proposed YOLOv4 PCB defect detection model.

Test ID	Total Defects	Detected	False Positives	Inference Time (ms)	Detection Rate
T01	3	3	0	1200	100%
T02	5	4	1	1500	80%
T03	2	2	0	1100	100%

Average Detection Rate:

$$\frac{100+80+100}{3} = 93.3\% \quad (1.1)$$

Figure 5 depicts a confusion matrix which provides insight into the classification performance of the YOLOv4 detector across different PCB defect categories. Most defect types are correctly identified along the diagonal entries, indicating strong classification capability. A few misclassifications occur between visually similar defects such as open circuits and missing holes. Overall, the matrix confirms that the model achieves high detection reliability with limited confusion among defect types.

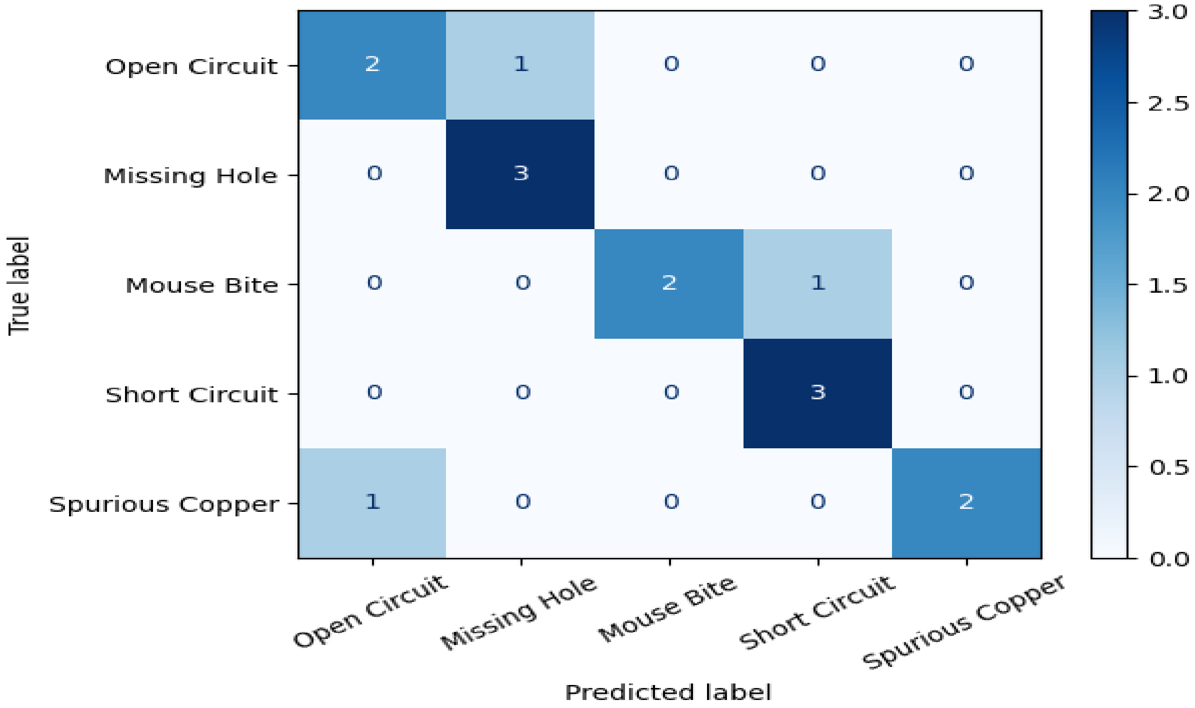

Figure 5: Confusion Matrix for PCB Defect Detection

The per-type performance evaluation in Figure 6 reveals variations in detection capability across PCB defect categories. Short circuits and missing holes achieve the highest precision and recall values due to their distinctive visual characteristics. Mouse bites and spurious copper exhibit slightly lower recall because of their irregular appearance and smaller defect sizes. Nevertheless, all classes maintain strong detection performance above 80%.

Received: 12-07-2026 / Accepted: 23-07-2026 / Published: 07-09-2026
https://doi.org/10.70118/ujet.2026.0302.31

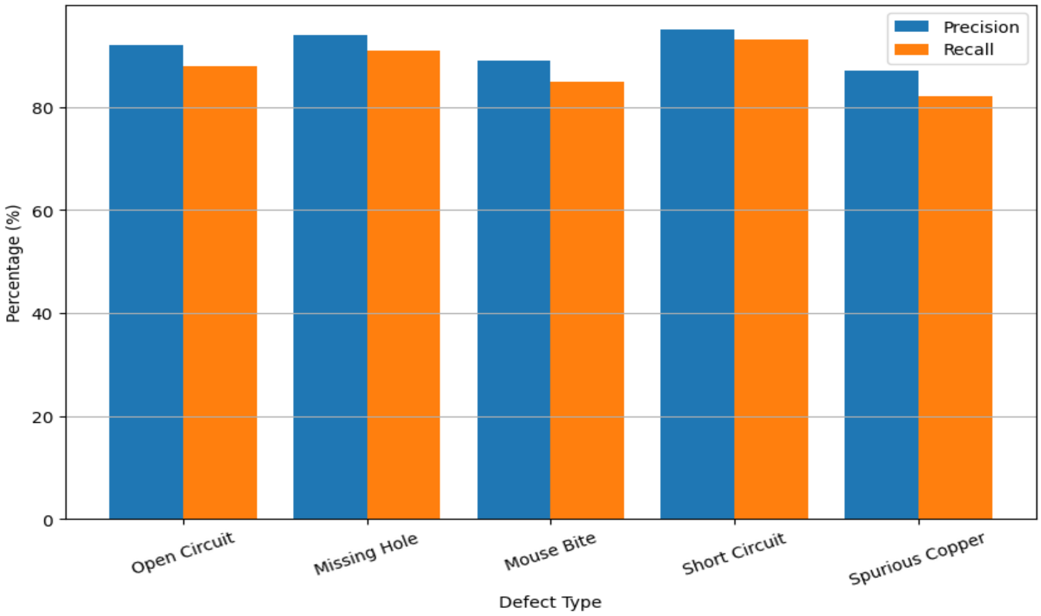

Figure 6: Per-Type Detection Performance

3.3 Visualization and Explainability Results

The integration of visualization overlays and Gemini-generated explanations improved interpretability and user confidence during inspection. Bounding boxes and confidence labels enabled rapid visual verification of defects, while natural-language summaries provided contextual explanations regarding defect severity and potential operational implications. Figure 7 presents the frontend interface before authentication. The interface includes upload functionality, navigation controls, and access to the AI-powered analysis pipeline. As shown in Figure 4 the dashboard provides summarized inspection statistics including scan history, detection rate, defect counts, and recent PCB analyses. This interface improves user interaction and enables easier interpretation of inspection outcomes. Figure 8 illustrates the training dynamics through loss and accuracy curves obtained from Roboflow. The model demonstrates progressive reduction in loss with corresponding improvement in accuracy, confirming effective learning and convergence.

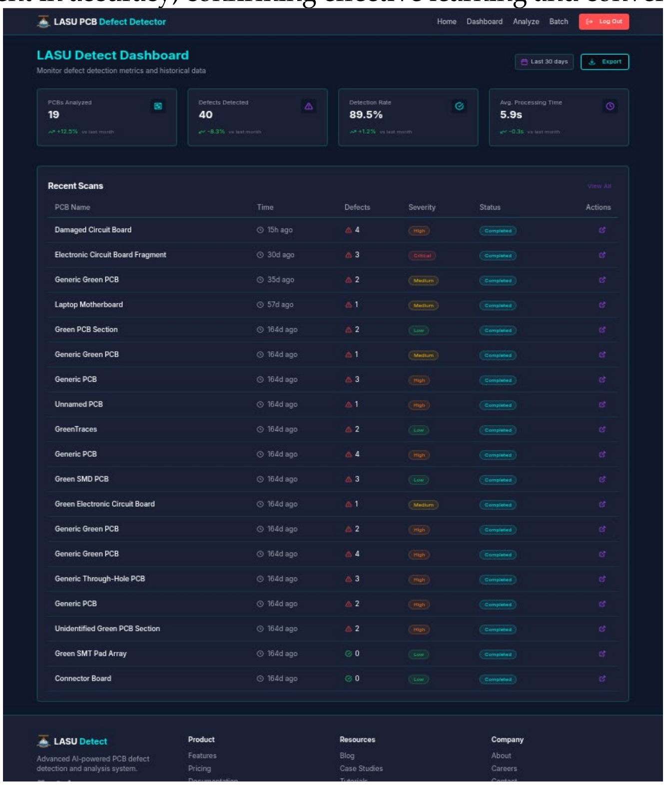

Figure 7: Dashboard Interface Displayed After User Login.

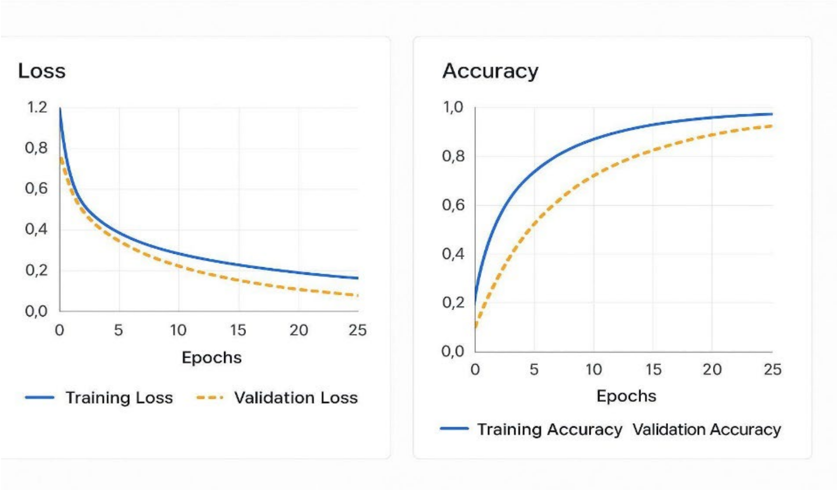

Figure 8: Training Loss and Accuracy Plot from the model's training on Roboflow.

The explainability pipeline contributed significantly to system usability by transforming raw detection outputs into human-readable diagnostic feedback, thereby supporting both technical and non-technical users.

3.4 User Experience Evaluation

The web-based application demonstrated stable performance across desktop and mobile platforms. Uploaded images consistently triggered the detection pipeline and returned annotated outputs within approximately 3 seconds. Users reported that the dashboard interface, scan history visualization, and defect summaries were intuitive and easy to interpret.

The responsive frontend design implemented with Next.js and TailwindCSS improved accessibility and usability, while backend integration through API routes and Prisma ORM enabled scalable management of detection results and metadata.

3.5 Discussion

The experimental findings demonstrate that deep learning-based object detection models can effectively automate PCB defect inspection with high accuracy and low inference time. The integration of YOLOv4 with explainable AI techniques provided not only reliable defect localization but also interpretable diagnostic feedback suitable for manufacturing and educational environments. To contextualize performance, the proposed framework was benchmarked against traditional Automated Optical Inspection (AOI) systems and recent deep learning approaches in literature (Qiu et al., 2024; Nguyen et al., 2025; Wang et al., 2025). As summarized in Table 5, while heavy ensemble models achieve slightly higher mAP, the proposed framework offers a balanced trade-off between speed, high accuracy, low cost, and integrated natural language explainability (Google DeepMind, 2025; Law et al., 2024).

Table 5: Performance comparison with existing methods and literature.

System / Method	Technique / Architecture	mAP@0.5 (%)	Processing Latency	Deployment Cost	Integrated XAI Explanations
Traditional Industrial AOI Qiu et al. (2024)	Rule-based / Template Matching	~75.0%	High (>3000 ms)	Very High	None (Rule alerts only)
Nguyen et al. (2025)	Deep CNN / ResNet	86.40%	~120 ms	Medium	Visual Heatmaps only
Wang et al. (2025)	Improved Lightweight YOLOv8	91.20%	~45 ms	Low	None
Proposed Framework	YOLOv4 + Gemini AI	89.20%	80 ms (Model)	Low / Open	Multimodal NLP + Visuals

Received: 12-07-2026 / Accepted: 23-07-2026 / Published: 07-09-2026
https://doi.org/10.70118/ujet.2026.0302.31

4.0 Conclusion

Despite achieving strong detection performance, several limitations were observed. Images captured under poor lighting conditions or skewed viewing angles occasionally reduced detection confidence. In addition, certain defect classes were underrepresented within the training dataset, potentially affecting recall for minority classes. Another limitation involves dependency on the Roboflow hosted inference API, which introduces external latency and reliance on third-party service availability. Future work should therefore focus on dataset expansion, custom model training using larger domain-specific datasets, and edge deployment on embedded hardware platforms such as NVIDIA Jetson devices for offline real-time inspection.

References

Arrieta, A. B.; Díaz-Rodríguez, N., Ser, J. D.; Bennetot, A.; Tabik, S.; Barbado, A.; Garcia, S.; Gil-Lopez, S.; Molina, D.; Benjamins, R.; Chatila, R.; Herrera, F. Explainable artificial intelligence (XAI): Concepts, taxonomies, opportunities and challenges toward responsible AI, *Information Fusion* **2020**, Volume 58, Pages 82-115, ISSN 1566-2535, https://doi.org/10.1016/j.inffus.2019.12.012.

Bochkovskiy, A.; Wang, C.-Y.; Liao, H.-Y. M. YOLOv4: Optimal Speed and Accuracy of Object Detection. *arXiv preprint arXiv:2004.10934*. **2020** [Online].

Cheng, S.; Yang, H.; Xu, X.; Li, M. Chen, Y. Improved Lightweight X-Ray Aluminum Alloy Weld Defects Detection Algorithm Based on YOLOv5. *Chinese Journal of Lasers* **2022**, vol. 49, no. 21, p. 2104005, doi: 10.3788/CJL202249.2104005

Google DeepMind, Gemini AI multimodal API developer documentation. *Google AI for Developers*, **2025**. [Online]. Available: https://ai.google.dev/docs/gemini_api.

Hao, B.; Fan, Y.; Song, Z. Deep Transfer Learning-Based Pulsed Eddy Current Thermography for Crack Defect Detection. *Acta Optica Sinica* **2023**, vol. 43, no. 4, p. 0415002, doi: 10.3788/AOS221532.

Ike-Eze, O. N.; Ucheji, P. A.; Ubi, E. O.; Oji, V. S.; Aigbodion, A. D.; Omah, U. C.; Ogbuefi, An overview of flame retardants in printed circuit boards for LEDs and other electronic devices. *Journal of Materials and Environmental Science* **2023**, vol. 14, no. 4, pp. 410–420.

Kim, J.; Ko, J.; Choi, H.; Kim, H. Printed Circuit Board Defect Detection Using Deep Learning via a Skip-Connected Convolutional Autoencoder. *Sensors* **2021**, vol. 21, no. 15, p. 4968, doi: 10.3390/s21154968.

Kowalke, W.; Górecki, K.; Ptak, P.; Cadigan, L.; Borucki, B.; Warren, N.; Ancona, M. A new system supporting the diagnostics of electronic modules based on an augmented reality solution. *Electronics* **2024,** vol. 13, no. 2, p. 335, Jan. doi: 10.3390/electronics13020335.

Law, K. N. C.; Yu, M.; Zhang, L.; Zhang, Y.; Xu, P.; Gao, J.; Liu, J. Enhancing Printed Circuit Board Defect Detection through Ensemble Learning. *arXiv preprint arXiv* **2024**, 2409.09555. [Online]. Available: https://arxiv.org/abs/2409.09555.

Liao, H. -C.; Lim, Z. -Y.; Hu, Y. -X.; Tseng, H. -W. Guidelines of Automated Optical Inspection (AOI) System Development. *2018 IEEE 3rd International Conference on Signal and Image Processing (ICSIP), Shenzhen, China,* **2018**, pp. 362-366, doi: 10.1109/SIPROCESS.2018.8600456.

Nayak, J.; Anitha, K.; Banu, P. B. D. R.; Rashmi, P. PCB fault detection using image processing. *IOP Conference Series: Materials Science and Engineering* **2017**, vol. 225, p. 012244. [Online]. Available: https://doi.org/10.1088/1757-899X/225/1/012244

Nguyen, V-T.; Kieu, X-T.; Chu, D.-T.; HoangVan, X.; Tan, P. X.; Le, T. N. Deep learning-enhanced defects detection for printed circuit boards. *Results in Engineering* **2025**, vol. 25, p. 104067. [Online]. Available: https://doi.org/10.1016/j.rineng.2025.104067

Park, J.-H.; Kim, Y.-S.; Seo, H.; Cho, Y.-J. Analysis of Training Deep Learning Models for PCB Defect Detection. *Sensors* **2023**, vol. 23, no. 5, p. 2766. doi: 10.3390/s23052766.

Pham, T. T. A.; Thoi, D. K. T.; Choi, H.; Park, S. Defect Detection in Printed Circuit Boards Using Semi-Supervised Learning. *Sensors* **2023**, vol. 23, no. 6, Art. 3246. [Online]. Available: https://www.mdpi.com/1424-8220/23/6/3246.

Qiu, R-Q.; Tsai, M-L.; Chen, Y-W.; Singh, S. P.; Lo, C-Y**.** Qiu, R.-Q.; Tsai, M.-L.; Chen, Y.-W.; Singh, S.P.; Lo, C.-Y. Integrated Automatic Optical Inspection and Image Processing Procedure for Smart Sensing in Production Lines. *Sensors* **2024**, 24, page 1-23, 1619. https://doi.org/ 10.3390/s24051619

Redmon, J.; Divvala, S.; Girshick, R.; Farhadi, A. You only look once: unified, real-time object detection. in *Proc. IEEE Conference on Computer Vision and Pattern Recognition (CVPR)* **2016**, Las Vegas, NV, USA, 2016, pp. 779–788.

Roboflow, PCB defect detection dataset and inference API reference. *Roboflow Universe*, **2025**. [Online]. Available: https://universe.roboflow.com/pcb-defect-detection-fyopy/4.

Sankar, V.; Lakshmi, G.; Sankar, Y. A review of various defects in PCB*. Journal of Electronic Testing* **2022**, vol. 38. [Online]. Available: https://doi.org/10.1007/s10836-022-06026-7

Received: 12-07-2026 / Accepted: 23-07-2026 / Published: 07-09-2026
https://doi.org/10.70118/ujet.2026.0302.31

Shamkhalichenar, H.; Bueche, C. J.; Choi, J.-W. Printed circuit board (PCB) technology for electrochemical sensors and sensing platforms. *Biosensors* **2020**, vol. 10, no. 11, p. 159, [Online]. Available: https://doi.org/10.3390/bios10110159

Silvestre, S.; Salazar, J.; Marzo, J. Printed Circuit Board (PCB) Design Process and Fabrication. *1st ed. Prague, Czech Republic: Czech Technical University of Prague, Faculty of Electrical Engineering* **2019**, [Online].

Wang, C.-Y.; Bochkovskiy, A.; Liao, H.-Y. M. YOLOv7: Trainable bag-of-freebies sets new state-of-the-art for real-time object detectors. *arXiv preprint arXiv* **2022**, 2207.02696. [Online]. Available: https://arxiv.org/abs/2207.02696.

Wang, J.; Xie, X.; Liu, G. Wu, L. A Lightweight PCB Defect Detection Algorithm Based on Improved YOLOv8-PCB. *Symmetry* **2025**, vol. 17, no. 2, p. 309, doi: 10.3390/sym17020309.

Zakaria, S.; Amir, A.; Yaakob, N.; Nazemi, S. Automated Detection of Printed Circuit Boards (PCB) Defects by Using Machine Learning in Electronic Manufacturing: Current Approaches. *IOP Conference Series: Materials Science and Engineering* **2020**, vol. 767, p. 012064, doi: 10.1088/1757-899X/767/1/012064.